

Short communication

## An approach to $Y_2O_3:Eu^{3+}$ optical nanostructured ceramics

R.P. Yavetskiy<sup>a,\*</sup>, V.N. Baumer<sup>a</sup>, N.A. Dulina<sup>a</sup>, Yu.I. Pazura<sup>a</sup>, I.A. Petrusha<sup>b</sup>, V.N. Tkach<sup>b</sup>,  
A.V. Tolmachev<sup>a</sup>, V.Z. Turkevich<sup>b</sup>

<sup>a</sup> STC “Institute for Single Crystals”, NAS of Ukraine, 60 Lenin Ave., 61001 Kharkov, Ukraine

<sup>b</sup> Institute for Superhard Materials, NAS of Ukraine, 2 Avtozavodskaya Str., 04074 Kyiv, Ukraine

Received 11 May 2011; received in revised form 15 August 2011; accepted 29 August 2011

Available online 5 October 2011

### Abstract

$Y_2O_3:Eu^{3+}$  (1 at.%) translucent nanostructured ceramics with total forward transmission achieving  $\sim 70\%$  of the theoretical limit has been obtained by the transformation-assisted consolidation of custom-made cubic  $Y_2O_3:Eu^{3+}$  nanopowders under high pressure (HP). Sintering under the pressure of 7.7 GPa and temperatures in the 100–500 °C range leads to the partial cubic-to-monoclinic phase transition that results in two-phase  $Y_2O_3:Eu^{3+}$  nanoceramics. The average grain size of ceramics  $d \leq 50$  nm for both  $Y_2O_3:Eu^{3+}$  polymorph is comparable with crystallite size of initial nanopowders ( $d \sim 40$  nm), indicating that the grain growth factor is near unity. The phase compositions, morphology, densities, preliminary optical and luminescent properties of synthesized nanostructured ceramics have been studied.

© 2011 Elsevier Ltd. All rights reserved.

PACS: 81.05.Je; 81.07.Bc; 81.20.Ev; 81.40.Vw

Keywords:  $Y_2O_3$ ; Sintering; Optical properties; Functional applications

### 1. Introduction

Strategy to influence the physical properties of bulk materials through control of their structure and composition on the nanoscale offers several advantages to preparation of optical ceramics materials for different applications (photonics, laser, scintillation technique). These advantages include improved mechanical properties, highly desirable in laser application, lower light scattering on defects (pores, inclusions, secondary phases) which dimension is below the wavelength of visible light, and possibility to create transparent materials even with non-cubic structure.<sup>1</sup> To form optical nanoceramics one should provide near theoretical density of consolidated material ( $>99.9\%$ ), high perfection of grain boundaries and low residual porosity while retaining the grain size at nanolevel. Conventional ceramic techniques, such as hot isostatic pressing and vacuum sintering, are unsuitable for production of nanoceramics due to competition of sintering and recrystallization processes at high temperatures required to complete remove the residual

porosity. For this reason several rapid sintering methods were developed to produce translucent/transparent nanostructured ceramics, namely current activated sintering technique,<sup>2,3</sup> high-pressure torsion method<sup>4</sup> and low-temperature HP sintering.<sup>5–7</sup>

Transformation-assisted consolidation of low-agglomerated nanopowders is one of the most efficient approaches to form bulk nanoceramics due to considerable activation of plastic flow during phase transition.<sup>8</sup> The sintering is greatly enhanced when the phase transformation is accompanied with specific volume decrease. HP usually reduce diffusion rate that permits to control the grain size of ceramics. Conversion of cubic  $Y_2O_3$  (C) into monoclinic modification (B) under HP is accompanied by formation of more close-packed structure (the relative volume decrease during phase transition is 7% per formula unit<sup>9</sup>), hence this process is beneficial for production of optical nanoceramics. Despite numerous publication on  $Y_2O_3$  highly transparent coarse-grained ceramics (see for example<sup>10</sup> and references therein), only few works describe obtaining of dense nanostructured ceramics  $Y_2O_3$ ,<sup>11–13</sup> however no evidence on their transparency was presented. Transparent  $Y_2O_3$  ceramics produced in<sup>14</sup> is rather submicron-grained than nanograined. In this letter we report for the first time  $Y_2O_3:Eu^{3+}$  translucent nanostructured ceramics, a promising optical material for

\* Corresponding author. Tel.: +380 57 341 0415; fax: +380 57 340 9343.  
E-mail address: [yavetskiy@isc.kharkov.ua](mailto:yavetskiy@isc.kharkov.ua) (R.P. Yavetskiy).

scintillators and phosphors,<sup>15,16</sup> obtained by transformation-assisted consolidation of nanopowders under HP.

## 2. Experimental procedure

Cubic  $\text{Y}_2\text{O}_3:\text{Eu}^{3+}$  (1 at.%) nanocrystalline powders were obtained by chemical co-precipitation from water solution. Yttrium and europium nitrates were used as the starting materials and  $(\text{NH}_2)_2\text{CO}$  as a precipitant. The formed precipitate was collected, filtered, washed several times with water and absolute ethanol, and dried in air at  $T=25^\circ\text{C}$ . Then the powders were grinded and calcined in the 700–1200 °C temperature range for 2 h. The consolidation of nanopowders was carried out by sintering under the 7.7 GPa pressure in the 25–500 °C temperature range for 1–20 min using a toroid type high pressure (HP) apparatus.<sup>17</sup> Before placing in the HP cell the initial nanopowders were uniaxially compacted into pellets under the 250 MPa pressure up to the density of 50–55% from the theoretical one.

The density of consolidated samples was estimated by standard Archimedes method. Phase identification was performed via X-ray diffraction (XRD) method on a SIEMENS D-500 X-ray diffractometer (CuK $\alpha$  radiation, graphite monochromator). The phases were identified using JCPDS PDF-1 card file and EVA retrieval system included in diffractometer software. Rietveld refinement was performed with FullProf program.<sup>18</sup> Average apparent size of crystallites was calculated with FullProf using powder pattern of LaB<sub>6</sub> for obtaining of instrumental profile function. The ceramics microstructure was studied by scanning electron microscopy (SEM) in secondary electrons on a Zeiss EVO 50XVP microscope. Optical measurements of ceramics were conducted with 1.55 mm thick pellets polished on both surfaces. The total transmittance in the 250–1100 nm wavelength range was determined using a Perkin-Elmer “LAMBDA-35” spectrophotometer equipped with an integration sphere. The luminescence was studied on an automated SDL-2 setup (LOMO) under excitation with a REIS-I X-ray tube (Cu anticathode,  $U=30\text{ kV}$ ) at room temperature.

## 3. Results and discussion

Fabrication of optical nanoceramics starts with non-agglomerated nanocrystalline powders. The initial  $\text{Y}_2\text{O}_3:\text{Eu}^{3+}$  powders had specific surface of 16–17 m<sup>2</sup>/g and consisted of near isolated particles of 40 nm in diameter and standard deviation in size distribution of 10%. Fig. 1 shows the results of Rietveld refinement (FullProf program<sup>18</sup>) for a grinded pellet of the nanostructured ceramics obtained under  $\sim 7.7\text{ GPa}$  and 100 °C. Initial nanopowder was cubic with average crystallite size of  $d_{\text{XRD}}=37.1\text{ nm}$ , whereas nanoceramic is two-phase and contains a mixture of cubic and monoclinic  $\text{Y}_2\text{O}_3:\text{Eu}^{3+}$  (Table 1). Initial data on monoclinic  $\text{Y}_2\text{O}_3$  for the Rietveld refinement were taken from Ref. 19. According to XRD analysis results, the partial C  $\rightarrow$  B phase transition starts in  $\text{Y}_2\text{O}_3:\text{Eu}^{3+}$  nanopowders under 7.7 GPa pressure, in good agreement with data for coarse powders.<sup>20</sup> Monoclinic yttria remains in the sintered ceramics under ambient pressure as a metastable phase.

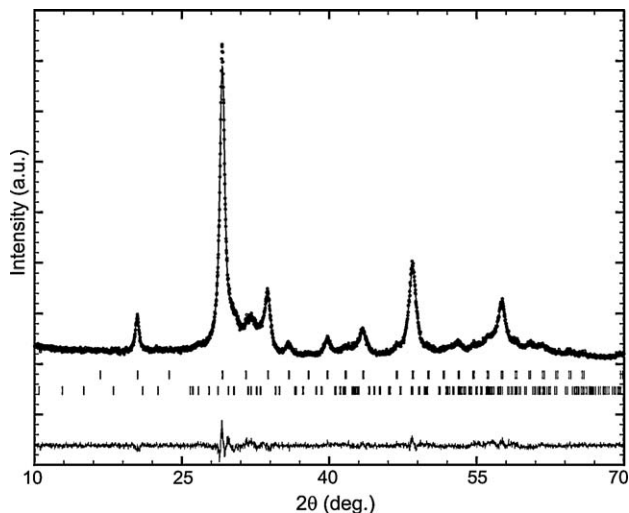


Fig. 1. Results of Rietveld refinement for  $\text{Y}_2\text{O}_3:\text{Eu}^{3+}$  (1 at.%) nanostructured ceramics. Upper and lower rows of vertical bars show the Bragg position of reflections for cubic and monoclinic phases, respectively.

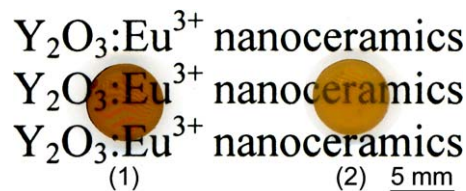


Fig. 2.  $\text{Y}_2\text{O}_3:\text{Eu}^{3+}$  (1 at.%) nanostructured ceramics obtained under  $P=7.7\text{ GPa}$  and  $T=300^\circ\text{C}$  (1) and  $200^\circ\text{C}$  (2). The pellets are 1.55 mm thick.

$\text{Y}_2\text{O}_3:\text{Eu}^{3+}$  cubic-to-monoclinic phase transition is kinetically controlled,<sup>9</sup> thus both sintering temperature and sintering time increase resulting in higher content of the monoclinic phase (45% and 80% for  $T=100^\circ\text{C}$  and  $300^\circ\text{C}$ , respectively). The typical parameters of  $\text{Y}_2\text{O}_3:\text{Eu}^{3+}$  nanopowders and nanoceramics are listed in Table 1. The crystallite size of the monoclinic  $\text{Y}_2\text{O}_3:\text{Eu}^{3+}$  was always lower than that of C- $\text{Y}_2\text{O}_3$ , indicating that nucleation prevails over nuclei growth. As can be seen, the microstrains observed in sintered ceramics are relatively low.

Fig. 2 illustrates a typical  $\text{Y}_2\text{O}_3:\text{Eu}^{3+}$  nanoceramics obtained in optimized quasi-hydrostatic conditions. The samples have yellowish-brown coloration related to the presence of color centers generated by reducing conditions during HP sintering. Various color centers are known to produce strong absorption in  $\text{RE}_2\text{O}_3$  (RE=Y, Sc, Lu) crystals, for instance, F-like centers (one or two electrons trapped by oxygen vacancy).<sup>21</sup> The coloration becomes deeper while increasing sintering temperature and time. The samples obtained at  $T \leq 100^\circ\text{C}$  contained a large concentration of submicron pores due to incomplete densification, and were opaque. Ceramics sintered at  $500^\circ\text{C}$  was black and non-transparent due to high concentration of color centers. Density of ceramics consolidated in the optimal sintering temperature range of 200–300 °C under  $P=7.7\text{ GPa}$  is  $5.2 \pm 0.2\text{ g/cm}^3$ , and lies between the theoretical values for cubic ( $5.03\text{ g/cm}^3$ ) and monoclinic  $\text{Y}_2\text{O}_3$  ( $5.41\text{ g/cm}^3$ ). Outside this temperature range density of ceramics noticeably decreases.  $\text{Y}_2\text{O}_3:\text{Eu}^{3+}$  transparent nanostructured ceramics is

Table 1  
Rietveld refinement results of  $\text{Y}_2\text{O}_3:\text{Eu}^{3+}$  nanopowders and nanoceramics.

Sample	Phase composition	Lattice parameters	Crystallite size $d_{\text{XRD}}$ , nm	Microstrains $\varepsilon$ , %
$\text{Y}_2\text{O}_3:\text{Eu}^{3+}$ (1 at.%) nanopowders	C- $\text{Y}_2\text{O}_3:\text{Eu}^{3+}$ 100%	sp.gr. $Ia\bar{3}$ $a = 10.60402(14) \text{ \AA}$ $V = 1192.37(3) \text{ \AA}^3$	37.1	0.0095
$\text{Y}_2\text{O}_3:\text{Eu}^{3+}$ (1 at.%) nanoceramics ( $P = 7.7 \text{ GPa}$ , $T = 100 \text{ }^\circ\text{C}$ )	C- $\text{Y}_2\text{O}_3:\text{Eu}^{3+}$ 56.5(7)%	sp.gr. $Ia\bar{3}$ $a = 10.6190(5) \text{ \AA}$ $V = 1197.44(1) \text{ \AA}^3$	39	0.87
	B- $\text{Y}_2\text{O}_3:\text{Eu}^{3+}$ 43.5(9)%	sp.gr. $C2/m$ $a = 14.026(5) \text{ \AA}$ $b = 3.5188(10) \text{ \AA}$ $c = 8.601(3) \text{ \AA}$ $\beta = 100.59(3)^\circ$ $V = 417.3(3) \text{ \AA}^3$	9	1.7

produced at extremely low temperatures ( $\sim 0.1$  of yttria melting point,  $T_m = 2440 \text{ }^\circ\text{C}$ ). A considerable decrease of temperatures required for the obtaining of dense ceramics is caused by the activation of the compaction process due to C  $\rightarrow$  B pressure-induced phase transition, probably, via active movement of particles as a whole, grain sliding and accommodation mechanisms.<sup>8</sup>

According to SEM data,  $\text{Y}_2\text{O}_3:\text{Eu}^{3+}$  nanoceramics is characterized by fine crystalline microstructure (Fig. 3). For the consolidation conditions studied the average grain size of ceramics ( $d \leq 50 \text{ nm}$  for both C- and B- $\text{Y}_2\text{O}_3:\text{Eu}^{3+}$ ) is comparable with crystallite size of initial nanopowders ( $d \sim 40 \text{ nm}$ ), indicating that the grain growth factor was  $\sim 1$ . The submicron and micron-sized porosity is entirely absent in the sintered material, but some residual nanoscale pores with characteristic size of  $\sim 30 \text{ nm}$  were observed (Fig. 3). The pores are uniformly distributed in the volume of sintered ceramics. Residual porosity greatly influences the optical properties of ceramics due to large difference in refractive index between the ceramics and gas-filled pores. The maximal scattering occurs when the pore size is equal to the wavelength of incident light.<sup>2</sup> However, in our samples the pore size is too small to produce significant scattering.

The optical transmittance and X-ray excited luminescence spectra of  $\text{Y}_2\text{O}_3:\text{Eu}^{3+}$  ceramics with thickness of 1.55 mm are presented in Fig. 4. The total forward transmission of  $\text{Y}_2\text{O}_3:\text{Eu}^{3+}$

ceramics is 55% at 1100 nm that achieves  $\sim 70\%$  of the theoretical limit of 82% (Fig. 4a). The theoretical simulations predicts that the residual porosity less than 0.1%, pore size below some critical limit (10 nm) and homogenous pore distribution are required to obtain optical transmittance comparable with that of single crystals.<sup>2</sup> Several factors contribute to decrease the optical transmittance of  $\text{Y}_2\text{O}_3:\text{Eu}^{3+}$  nanoceramics in comparison with single crystals. (1) The residual porosity with pore size of 30 nm increases the fraction of back-scattered light. (2) The color centers effectively absorb incident radiation (various color centers in  $\text{RE}_2\text{O}_3$  single crystals have absorption coefficients of about tens of  $\text{cm}^{-1}$ <sup>20</sup>). (3) The presence of several phases with different refractive indexes results in scattering of incident light

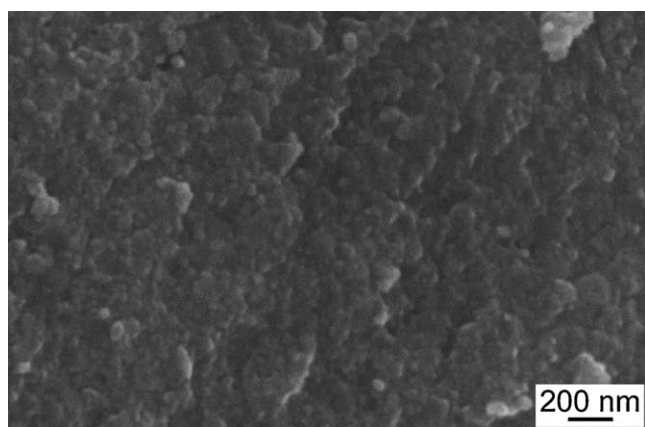


Fig. 3. SEM image of the polished surface of  $\text{Y}_2\text{O}_3:\text{Eu}^{3+}$  (1 at.%) ceramics obtained at  $P \sim 7.7 \text{ GPa}$  and  $T = 200 \text{ }^\circ\text{C}$ .

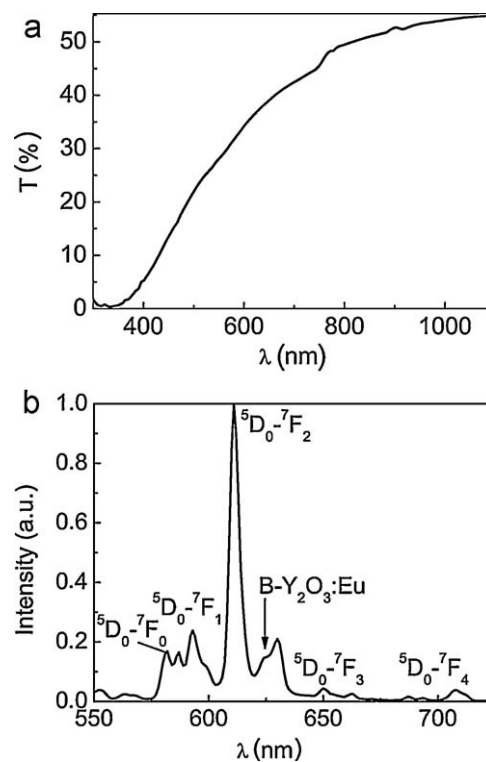


Fig. 4. Total forward transmittance (a) and normalized luminescence spectrum excited by X-rays (b) of  $\text{Y}_2\text{O}_3:\text{Eu}^{3+}$  (1 at.%) nanoceramics. The arrow indicates the most intense luminescence line of B- $\text{Y}_2\text{O}_3:\text{Eu}^{3+}$ .

at the grain boundaries. A red shift of fundamental absorption is caused by formation of Eu-O charge transfer band or by absorption of color centers since cubic and monoclinic  $Y_2O_3$  have almost the same band gaps  $E_g \approx 4.5$  eV.<sup>9</sup>

Luminescence of  $Y_2O_3:Eu^{3+}$  ceramics under X-ray excitation is presented by the group of the lines in the  $\lambda = 550$ – $720$  nm range with a maximum at  $\lambda = 611$  nm (Fig. 4b). The structure of luminescence spectra differs only slightly with consolidation conditions and agrees with those for initial nanopowders.  $Eu^{3+}$  ions in cubic and monoclinic  $Y_2O_3$  polymorphs demonstrate different luminescence spectra due to various crystallographic environments. Cubic  $Y_2O_3$  has 2 independent position for europium ions, the emission originates mainly from europium ions in  $C_2$  site ( $^5D_0 \rightarrow ^7F_J$  ( $J=0-4$ ) transitions). In the monoclinic  $Y_2O_3$  europium ions occupy three independent positions and produce luminescence in the 575–715 nm wavelength range with a maximum at 624 nm corresponding to  $^5D_0 \rightarrow ^7F_2$  transition (a shoulder indicated by arrow in the luminescence spectrum, Fig. 4b). Thus emission of  $Y_2O_3:Eu^{3+}$  is a superposition of X-ray excited luminescence of  $Eu^{3+}$  ions in the cubic and monoclinic modifications, herein, contribution from radiative transitions in C- $Y_2O_3$  is predominant. Luminescence of B- $Y_2O_3:Eu^{3+}$  at room temperature is partially quenched. This is due to europium ions in monoclinic  $Y_2O_3$  are mainly situated in perturbed positions (near grain boundaries), since crystallite size of B- $Y_2O_3:Eu^{3+}$  is extremely small ( $d_{XRD} = 9$  nm). The detailed results on luminescent studies of  $Y_2O_3:Eu^{3+}$  nanostructured ceramics will be published elsewhere.

#### 4. Conclusions

To conclude,  $Y_2O_3:Eu^{3+}$  (1 at.%) optical nanostructured ceramics with total transmittance of 55% at 1100 nm for 1.55 mm thick sample has been produced by transformation-assisted sintering under  $P = 7.7$  GPa and temperature as low as  $0.1T_m$ . Dense ceramics consists on a mixture of cubic and monoclinic phases with the typical grain size of  $\sim 50$  nm, comparable with crystallite size of initial nanopowders. Under X-ray excitation  $Y_2O_3:Eu^{3+}$  ceramics shows orange-red luminescence connected mainly with  $^5D_0 \rightarrow ^7F_J$  ( $J=0-4$ ) transitions of  $Eu^{3+}$  ions in the cubic yttria.

#### Acknowledgments

The work was partially supported by Target Complex Program of Fundamental Research of NAS of Ukraine “Fundamental problems of Nanostructured Systems, Nanomaterials and Nanotechnologies” # 76/07-H (Project “Spalakh”).

#### References

- Messing GL, Stevenson AJ. Toward pore-free ceramics. *Science* 2008;**322**:383–4.

- Anselmi-Tamburini U, Woolman JN, Munir ZA. Transparent nanometric cubic and tetragonal zirconia obtained by high-pressure pulsed electric current sintering. *Adv Funct Mater* 2007;**17**:3267–73.
- Casolco SR, Xu J, Garay JE. Transparent/translucent polycrystalline nanostructured yttria stabilized zirconia with varying colors. *Scripta Mater* 2008;**58**:516–9.
- Gizhevskii BA, Sukhorukov YuP, Ganshina EA, Loshkareva NN, Telegin AV, Lobachevskaya NI, et al. Optical and magneto-optical properties of nanostructured yttrium iron garnet. *Phys Solid State* 2009;**51**:1836–42.
- Zhang J, Lu T, Chang X, Wei N, Xu W. Related mechanism of transparency in  $MgAl_2O_4$  nano-ceramics prepared by sintering under high pressure and low temperature. *J Phys D: Appl Phys* 2009;**42**:052002 [5 pp.].
- Fedyk R, Hreniak D, Łojkowski W, Strek W, Matysiak H, Grzanka E, et al. Method of preparation and structural properties of transparent YAG nanoceramics. *Opt Mater* 2007;**29**:1252–7.
- Galceran M, Pujol MC, Gluchowski P, Strek W, Carvajal JJ, Mateos X, et al. A promising  $Lu_{2-x}Ho_xO_3$  laser nanoceramic: synthesis and characterization. *J Am Ceram Soc* 2010;**93**:3764–72.
- Ragulya AV. Consolidation of ceramic nanopowders. *Adv Appl Ceram* 2008;**107**:118–34.
- Yusa H, Tsuchiya T, Sata N, Ohshiz Y. Dense yttria phase eclipsing the A-type sesquioxide structure: high-pressure experiments and ab initio calculations. *Inorg Chem* 2010;**49**:4478–85.
- Jin L, Zhou G, Shimai S, Zhang J, Wang S.  $ZrO_2$ -doped  $Y_2O_3$  transparent ceramics via slip casting and vacuum sintering. *J Eur Ceram Soc* 2010;**30**:2139–43.
- Chen I-W, Wang X-H. Sintering dense nanocrystalline ceramics without final-stage grain growth. *Nature* 2000;**404**:168–71.
- Chaim R, Shlayer A, Estournes C. Densification of nanocrystalline  $Y_2O_3$  ceramic powder by spark plasma sintering. *J Eur Ceram Soc* 2009;**29**:91–8.
- Kear BH, Al-Sharab JF, Sadangi RK, Deutsch S, Kavukcuoglu NB, Tse SD, et al. On the conversion of bulk polycrystalline  $Y_2O_3$  into the nanocrystalline state. *J Am Ceram Soc* 2011;**94**:1744–6.
- Serivalsatit K, Yazgan Kokuoz B, Kokuoz B, Ballato J. Nanograined highly transparent yttria ceramics. *Opt Lett* 2009;**34**:1033–5.
- Fukabori A, Yanagida T, Pejchal J, Maeo S, Yokota Y, Yoshikawa A, et al. Optical and scintillation characteristics of  $Y_2O_3$  transparent ceramic. *J Appl Phys* 2010;**107**:073501 [6 pp.].
- Podowitz SR, Gaume R, Feigelson RS. Effect of europium concentration on densification of transparent  $Eu:Y_2O_3$  scintillator ceramics using hot pressing. *J Am Ceram Soc* 2010;**93**:82–8.
- Khvostantsev LG, Vereschagin LF, Novikov AP. Device of toroid type for high pressure generation. *High Temp High Pressures* 1977;**9**:637–9.
- Rodriguez-Carvajal J, Roisnel T. FullProf.98 and WinPLOTR: new Windows 95/NT applications for diffraction commission for powder diffraction. *IUCr Newsltt* 1998;**20**.
- Antić B, Mitrić M, Rodič D. Cation ordering in cubic and monoclinic  $(Y,Eu)_2O_3$ : an X-ray powder diffraction and magnetic susceptibility study. *J Phys: Condens Matter* 1997;**9**:365–74.
- Wang L, Pan Y, Ding Y, Yang W, Mao WL, Sinogeikin SV, et al. High-pressure induced phase transitions of  $Y_2O_3$  and  $Y_2O_3:Eu^{3+}$ . *Appl Phys Lett* 2009;**94**:061921 [3 pp.].
- Peters R, Petermann K, Hubert G. Growth technology and laser properties of Yb-doped sesquioxides. In: Capper P, Rudolph P, editors. *Crystal growth technology: semiconductors and dielectrics*. Weinheim: Wiley-VCH Verlag GmbH & Co. KGaA; 2010. p. 267–82.